Journal of Quantitative Spectroscopy & Radiative Transfer 161 (2015) 117–130

Contents lists available at ScienceDirect

Journal of Quantitative Spectroscopy & Radiative Transfer

journal homepage: www.elsevier.com/locate/jqsrt

# MARVEL analysis of the measured high-resolution spectra of $^{14}NH_3$

Afaf R. Al Derzi [a], Tibor Furtenbacher [b,c], Jonathan Tennyson [a,*], Sergei N. Yurchenko [a], Attila G. Császár [b,c]

[a] Department of Physics and Astronomy, University College London, Gower Street, London WC1E 6BT, UK
[b] Institute of Chemistry, Loránd Eötvös University, H-1117 Budapest, Pázmány sétány 1/A, Hungary
[c] MTA-ELTE Research Group on Complex Chemical Systems, H-1518 Budapest 112, P.O. Box 32, Hungary

ARTICLE INFO

*Article history:*
Received 4 February 2015
Accepted 24 March 2015
Available online 11 April 2015

*Keywords:*
Ammonia vapor
High-resolution spectroscopy
Rotation–vibration energy levels

ABSTRACT

Accurate, experimental rotational–vibrational energy levels and line positions, with associated labels and uncertainties, are reported for the ground electronic state of the symmetric-top $^{14}NH_3$ molecule. All levels and lines are based on critically reviewed and validated high-resolution experimental spectra taken from 56 literature sources. The transition data are in the 0.7–17 000 $cm^{-1}$ region, with a large gap between 7000 and 15 000 $cm^{-1}$. The MARVEL (Measured Active Rotational–Vibrational Energy Levels) algorithm is used to determine the energy levels. Out of the 29 450 measured transitions 10 041 and 18 947 belong to ortho- and para-$^{14}NH_3$, respectively. A careful analysis of the related experimental spectroscopic network (SN) allows 28 530 of the measured transitions to be validated, 18 178 of these are unique, while 462 transitions belong to floating components. Despite the large number of spectroscopic measurements published over the last 80 years, the transitions determine only 30 vibrational band origins of $^{14}NH_3$, 8 for ortho- and 22 for para-$^{14}NH_3$. The highest $J$ value, where $J$ stands for the rotational quantum number, for which an energy level is validated is 31. The number of experimental-quality ortho- and para-$^{14}NH_3$ rovibrational energy levels is 1724 and 3237, respectively. The MARVEL energy levels are checked against ones in the BYTe first-principles database, determined previously. The lists of validated lines and levels for $^{14}NH_3$ are deposited in the Supporting Information to this paper. Combination of the MARVEL energy levels with first-principles absorption intensities yields a huge number of experimental-quality rovibrational lines, which should prove to be useful for the understanding of future complex high-resolution spectroscopy on $^{14}NH_3$; these lines are also deposited in the Supporting Information to this paper.



## 1. Introduction

There are several reasons which can be given to explain why the structure [1–10] and the spectra [2,8,11–149] of the ammonia molecule have been the subject of a large number of experimental and theoretical investigations. In what follows we focus on spectroscopic issues most relevant for our own study presented here: (1) Ammonia is a simple, stable four-atomic chemical species. It is one of the principal deposits of nitrogen in molecules, it provides one of the most accurate "molecular thermometers" for the interstellar medium, and it is omnipresent in planet-forming primordial gas clouds. (2) Since ammonia contains

* Corresponding author.
*E-mail addresses:* j.tennyson@ucl.ac.uk (J. Tennyson), csaszar@chem.elte.hu (A.G. Császár).

http://dx.doi.org/10.1016/j.jqsrt.2015.03.034
0022-4073/

"only" four nuclei and 10 electrons, it is among the few polyatomic molecules for which sophisticated quantum chemical (electronic and nuclear motion) computations have become feasible during the last few decades. Therefore, potential energy surfaces (PESs) of varying accuracy have been derived for ammonia [8,75,102,103,106,109,111,118,126,127,133,134] and rotational–vibrational states of ever increasing accuracy and of ever increasing excitation have been computed. (3) The quantum chemical model of the ammonia molecule involves a characteristic large-amplitude motion called inversion, exhibiting a symmetric double-well potential [83,100,107,121,150]. The height of the effective barrier is $2021 \pm 20\ \mathrm{cm}^{-1}$, when relativistic effects (about $+20\ \mathrm{cm}^{-1}$), Born–Oppenheimer diagonal corrections (about $-10\ \mathrm{cm}^{-1}$), and zero-point vibrations (about $+244\ \mathrm{cm}^{-1}$) are all considered [20,100,150,151]. Treating the inversion motion is challenging for perturbative approaches and calls for fourth-age quantum chemical [152] nuclear motion treatments [131,153–156]. (4) The parent isotopologue of ammonia, $^{14}NH_3$, exists in two nuclear-spin isomer forms (Table 1), ortho (proton quartet) and para (proton doublet), which correspond to different values of the total nuclear spin ($I$) of the three H atoms [157]. The related nuclear-spin conversion in ammonia has been investigated in a number of publications [63,68,74,122] but has not been observed in high-resolution spectroscopic experiments. (5) Ammonia is poisonous and its ever-increasing release into the atmosphere of earth has undesirable consequences; thus, monitoring of ammonia in the atmosphere and a detailed understanding of the nitrogen cycle are particularly important scientific objectives. Remote sensing of spatially resolved atmospheric concentrations of ammonia requires reliable and extensive laboratory data. (6) Ammonia spectra are proving useful for metrology studies including accurate determination of the Boltzmann constant [136,141,143], determining the time variation of the electron-to-proton mass ratio [116,158], and other precision measurements [149].

These arguments are sufficient to explain why an attempt is made here to collect all the high-resolution experimental information available for $^{14}NH_3$, critically review and validate it, and determine experimental-quality rovibrational energy levels using the MARVEL (Measured Active Rotational–Vibrational Energy Levels) [159–163] protocol and code. Note that MARVEL has been used successfully to determine experimental-quality energy levels for nine water isotopologues [164–168], three $H_3^+$ isotopologues [169,170], and parent ketene [171] prior to being used here to obtain energy levels for $^{14}NH_3$ via a weighted linear least-squares fit.

**Table 1**
Spin statistical weights and symmetry characteristics of the rovibrational states of $^{14}NH_3$ based on the $D_{3h}$(M) molecular symmetry (MS) group.[a]

| $\Gamma_{\mathrm{rve}}$ | Statistical weight |
|---|---|
| $A_1'$ | 0 |
| $A_2'$ | 12 |
| $E'$ | 6 |
| $A_1''$ | 0 |
| $A_2''$ | 12 |
| $E''$ | 6 |

[a] Levels of species $A_2^{\dagger} := \{A_2', A_2''\}$ belong to ortho-$^{14}NH_3$, levels of species $E^{\dagger} := \{E', E''\}$ belong to para-$^{14}NH_3$ (by definition, ortho levels should have the higher spin statistical weights [157]), while levels of species $A_1^{\dagger} := \{A_1', A_1''\}$ are the so-called "missing" levels.

## 2. Theoretical background

### 2.1. The MARVEL protocol

The methods employed in this study for collecting and critically evaluating labelled experimental transition wavenumbers and their uncertainties and for inverting the transitions in order to obtain the best possible energy levels with corresponding uncertainties are based on the concept of spectroscopic networks [159,160,172] and on the MARVEL inversion-refinement procedure [159–163]. During a MARVEL analysis we simultaneously process *all* the available assigned and labelled experimental lines which yield, via a weighted linear least-squares inversion protocol, the associated energy levels. In MARVEL a robust reweighting scheme [173] is adopted, whereby uncertainties for selected line positions are changed (in practice increased) during the iterative refinement of the levels [161]. After removing outliers from the experimental transition data and applying the iterative robust reweighting algorithm, a database is created containing self-consistent and uniquely labelled transitions and improved uncertainties. The procedure is such that the final energy levels and their uncertainties are guaranteed to be compatible with the (adjusted) uncertainties of the experimental line positions. This means that all experimental transitions used in the MARVEL procedure agree, within their revised stated uncertainties, with the predicted transitions built upon the MARVEL energy levels. This criterion for the uncertainty is therefore more stringent than the usual standard deviation used to represent statistical error in experiments and will usually lead to the quoted MARVEL uncertainties being systematically larger.

After the data collection is completed, the first step in the MARVEL procedure is to split the transition data into components of the spectroscopic network (SN) [160], characterizing the molecule as well as the measured data. Components of the SN contain all interconnected rotational–vibrational energy levels supported by the grand database of the labelled transitions. For $^{14}NH_3$, the transitions must form two rooted, principal components (PC) [160], an ortho and a para one (Table 1). Other components of the SN whose nodes are unattached to either of the two PCs are designated as floating components (FCs). The absolute energies of the FCs cannot be determined in a MARVEL run, only the relative energies within a FC.

The second step of the MARVEL procedure involves the checking of all transitions for uniqueness of and errors in their labels. Conflicts arising from the transcription of the experimental data must be found and corrected at this stage.

The third step is the execution of the iterative weighted linear least-squares fit. The fit must be followed carefully to ensure the correctness of the energy levels. This involves occasional rechecking of the experimental data.

Finally, in the fourth step, the MARVEL energy levels, including their labels, are checked against first-principles results given in the BYTe first-principles linelist of $^{14}NH_3$ [174]. At this stage a few transitions yielding energy levels incompatible with clear trends observable between variational and MARVEL energy levels are removed.

### 2.2. Nuclear spin statistics

A valid basis function for expressing the complete internal motion wavefunction results from the combination of a rovibronic (rve) state having symmetry $\Gamma_{\rm rve}$ and a nuclear spin state, having symmetry $\Gamma_{\rm ns}$, whereby the direct product of the two symmetries is an allowed symmetry of the complete internal motion wavefunction, $\psi_{\rm int}$ [157]. In other words, the allowed states fulfill the $\Gamma_{\rm rve} \otimes \Gamma_{\rm ns} \supset \Gamma_{\rm int}$ relation.

The existence of nuclear spin states which do not have the allowed symmetry for combination with a particular rovibronic state introduces the concept of "missing" levels (see footnote to Table 1). Such rovibronic levels correspond to eigenvalues of the usually employed rovibronic Hamiltonians, but no transitions will originate from or end on them because of the symmetry restriction. $^{14}NH_3$ is a pyramidal molecule of the molecular symmetry group $D_{3h}$ [157]. The statistical weights given in Table 1 for $^{14}NH_3$ arise from the use of nuclear spins $I=1$ for $^{14}N$ and $I=\frac{1}{2}$ for $^{1}H$ and application of the Pauli principle to the identical, fermionic H atoms. The $A_1^{\dagger} := \{A_1', A_1''\}$ (ro)vibrational states are not allowed due to their zero nuclear spin statistical weight factors.

### 2.3. Quantum numbers and selection rules

It is a requirement of the MARVEL protocol that the input dataset contains a unique label for both the lower and the upper states involved in each transition so that the spectroscopic network corresponding to the union of the measurements can be built up unambiguously. There is no requirement that the labels have any physical significance, although this is desirable.

Due to the nature of the experimental transition data available for $^{14}NH_3$, issues were anticipated with the approximate rovibrational labels employed by the different experimental investigations. Many of the problems arising from the lack of an established and accepted set of quantum numbers for symmetric tops have recently been discussed in detail for $^{14}NH_3$ by some of us in 13DoHiYuTe [142]. In what follows we basically follow the recommendations of Ref. [142].

For consistency and to maintain a single set of uniform labels for all levels, we choose to label vibrational states in the usual normal-mode notation, $(v_1 v_2 v_3 l_3 v_4 l_4)$, where the corresponding $\nu_1$ and $\nu_2$ are the symmetric stretch and symmetric bend modes, respectively, and $l_3$ and $l_4$ are vibrational angular momentum quantum numbers corresponding to the doubly degenerate $\nu_3$ (asymmetric stretch) and $\nu_4$ (asymmetric bend) modes, respectively. Naturally, $l_m = -v_m, -v_m+2, \ldots, v_m-2, v_m$ with $m=3,4$. Furthermore, $l = l_3 + l_4$, where $l$ represents the total vibrational angular momentum. Following Ref. [142], we choose $L_3 = |l_3|$, $L_4 = |l_4|$, and $L = |l|$. None of the vibrational quantum numbers are good quantum numbers.

$^{14}NH_3$ is a symmetric-top rotor. The standard symmetric-top quantum numbers ($J$ $k$) are used as part of the label of the rovibrational states. Rotations are described by the rigorous quantum number $J$ and the rotational angular momentum quantum number $k$ (and $K = |k|$) corresponding to the projection of the rotational angular momentum $\mathbf{J}$ on the $C_3$ symmetry axis, $k = -J, \ldots, J$. Note that $k$ is not a good quantum number. Using $K$ in the label makes the definition of the rotational state incomplete. For example, BYTe uses rotational parity as an extra label, while 13DoHiYuTe [142] recommends $\Gamma_{\rm r}$.

Another descriptor employed is $i$, corresponding to the inversion symmetry of the $\nu_2$ vibrational motion, which can take values of 0 or 1 (symmetric, $s$, or asymmetric, $a$, respectively). The last triad of descriptors of an energy level is its vibrational, rotational, and total symmetry, represented by $\Gamma_{\rm v}$, $\Gamma_{\rm r}$, and $\Gamma_{\rm rv}$, respectively, spanning $A_1^{\dagger}$, $A_2^{\dagger}$, and $E^{\dagger}$.

In summary, as only the uniqueness of the labels of the energy levels is required for a MARVEL analysis, in the present study we decided to employ labels with redundant information to describe rotational–vibrational energy levels of $^{14}NH_3$. The rotation–vibration levels of $NH_3$ are thus identified by a set of altogether 12 descriptors: $(v_1\ v_2\ v_3\ v_4\ l_3\ l_4\ J\ K\ i\ \Gamma_{\rm r}\ \Gamma_{\rm v}\ \Gamma_{\rm rv})$. This set of descriptors is basically the same as that employed in 13DoHiYuTe [142], except that here $l_3$ and $l_4$ are used instead of $L_3$ and $L_4$, respectively. The present choice ensures that all labels used in MARVEL are unique, as required. Although for many low-lying states the quantum numbers chosen embody several redundancies, in "extreme" cases, involving multiple excitations in degenerate vibrations, only $i$ is not required to uniquely specify each state. Retention of $i$ was recommended in Ref. [142] because of the importance of the inversion mode. Variational nuclear motion computations, employed in this study extensively for validation and quality assurance, yield the rigorous descriptors $J$ and $\Gamma_{\rm rv}$ without difficulty; other approximate quantum numbers and symmetry descriptors can usually be extracted but this is not without difficulties. The vibrational and rotational labels are sometimes referred to as $(v_1\ v_2\ v_3^{l_3}\ v_4^{l_4})$ and $[J\ K]$, respectively.

Experimentalists prefer to label measured transitions as ${}^{\Delta K}\Delta J(J,K)_{s/a}$ or ${}^{\Delta K}\Delta J_K(J)$, and use the standard $P$, $Q$, $R$ notation for $\Delta K := K_{\rm f} - K_{\rm i} = -1, 0, +1$ and $\Delta J := J_{\rm f} - J_{\rm i} = -1$, $0, +1$, respectively. These labels were converted to the 12-element description defined above. We note that for a number of data sources it proved necessary to systematically relabel data as the published labels were inconsistent with and occasionally did not map into the 12 descriptors employed in this study.

Before processing the published transition data, we checked, as thoroughly as possible, whether the transition labels were correct, *i.e.*, correspond to the known selection rules [142], and consistent. The selection rules related to

approximate quantum numbers are based on symmetry relations. The explicit selection rules applicable for $NH_3$ are $\Delta J = 0, \pm 1$, $J' + J'' \geq 1$, $A_2' \leftrightarrow A_2''$ and $E' \leftrightarrow E''$. The symmetry selection rules give rise to a rule that $\Delta(k-l) = 3n$ with $n = 0, 1, 2, \ldots$ [175]; when applying this rule one needs to remember that each $K = 1, 2, 4, 5, 7, 8, \ldots$ comprises a degenerate pair $k = \pm K$ which means that, for example, transitions with $\Delta l = 0$ of the form $K' = 1 \leftarrow K'' = 2$ are allowed, since $1-(-2) = 3$, as well as $-1-(+2) = -3$ [69]. Ammonia shows a strong propensity to undergo transitions with $\Delta(k-l) = 0$ for transitions between states with $A_1^\dagger$ and $A_2^\dagger$ vibrational symmetry. If all transitions had this form, each value of $K$ would give rise to a distinct component of the SN of $^{14}NH_3$. However, the so-called "forbidden" transitions with $\Delta k = 3, 6, \ldots$ [45,69] can link these components; "forbidden" transitions therefore play a particularly important role in that they connect components which would otherwise be distinct.

Where possible, we corrected those descriptors of the labels which proved to be inconsistent among the many sources. To expedite this procedure, for many molecules help comes from rovibrational labels taken from computations based on the use of an effective Hamiltonian (EH). However, for the majority of the higher-lying energy levels, results from accurate EH computations are not available for $^{14}NH_3$. Validation of some of the labels attached to the observed transitions was thus performed as follows. Transitions were examined for consistency of the upper levels derived from combination difference (CD) relations. This method is a simple and powerful tool for the assignment of rovibrational spectra; however, it cannot be applied to transitions not part of several CD relations. All the transitions associated with a given rotational level of the vibrational ground state have been considered for combination differences. At this stage, conflicts in the labels could be traced and corrected. Many CD relations for other vibrational states have also been checked.

### 2.4. BYTe

Yurchenko et al. published two $^{14}NH_3$ linelists [174,176] and one for $^{15}NH_3$ [177], computed using variational nuclear motion procedures outlined below. The initial $^{14}NH_3$ linelist [176] is only valid for applications up to 300 K, while their hot $^{14}NH_3$ linelist [174], which they named BYTe, is more extensive, more accurate, and more useful for higher temperatures; thus, only BYTe will concern us here.

The BYTe linelist [174], composed of 1 373 897 energy levels and 1 138 323 351 transitions, was computed using the nuclear motion program TROVE [154], a spectroscopically determined potential energy surface [178], and an *ab initio* dipole moment surface [110]. Although BYTe offers a very extensive range of energy and associated transitions, with levels up to 18 000 $cm^{-1}$ and rotational states with $J \leq 36$, the underlying PES means that these levels become increasingly unreliable above about 5000 $cm^{-1}$. Above 5000 $cm^{-1}$ more accurate calculated energy levels are available from Huang et al. [118,179,180]; however, during these studies no transition intensities were computed and therefore they do not provide a linelist.

### 2.5. Vibrational labels

As mentioned above, the MARVEL procedure requires all states to be distinctly labelled in a consistent, if not necessarily physically meaningful, manner. Labelling of the energy levels of ammonia becomes complicated at higher energies and a small number of works considered here [57,95,96,148] make line assignments but do not provide a full set of labels for the upper vibrational state involved in the transition. Since these works provide valuable information on ammonia energy levels we attempted to provide vibrational labels so that the measured transitions could be included in our analysis. We would warn against ascribing too much physical meaning to these new labels.

In performing this labelling a distinction must be made between spectra which lie in the frequency range covered by the BYTe linelist and that of 86CoLe [57] which does not. For unlabelled transitions lying within the BYTe regions an attempt was made to label transitions either from other (labelled) experimental works or using BYTe, in which case BYTe labels were adopted. In what follows the labelling is discussed separately for each relevant source.

99KlBrTaKo [95] contains 138 partially assigned lines between 3010 and 3554 $cm^{-1}$. We were able to label 114 of these and regard the other 24 as unvalidated.

00CoKlTaBr [96] contains 22 partially labelled lines between 1423 and 1905 $cm^{-1}$. All of these lines could be labelled based on the information available from the other experimental sources and BYTe.

The cold spectrum given in 14FoGoHeSo [148] only contains vibrationally unlabelled transitions. We were able to label about half of the reported transitions based on our MARVEL analysis of all other sources. These transitions are included in the final MARVEL analysis.

For the visible wavelength spectra of 86CoLe [57] a somewhat different strategy was required to label the observed transitions. All lower states were assumed to belong to the ground vibrational state, $000^00^0$. Feasible upper-state vibrational labels were taken from BYTe and arranged in simple energy order. The vibrational labels were picked one by one to supplement the upper state label with the simple guiding principle to keep the number of distinct labels at a minimum. This method generated a self-consistent set of transitions with self-consistent labels but the vibrational labels chosen are without physical meaning. In the end we were able to label all the 323 transitions in 86CoLe using only 18 vibrational band origins (VBOs). A significant number of upper states could be confirmed by CD relations. We are thus confident of the upper state energies given by this procedure if not the labels.

## 3. Experimental data and data treatment

For $^{14}NH_3$, there exists a large number of at least partially assigned high-resolution experimental spectra [2,13,20,29–31,38,41,42,45,46,50–54,57,62,67,69,76,77,79,84–86,88,91,92,95,96,98,99,112,119,128–130,132,135,139,140,142,146,148]. The data from room-temperature measurements are augmented by data from a number of warm (373 K) [31,46], hot (up to 1640 K) [129,135,137,138], and

cold [93,148] spectra. Hot spectra are rich in high-$J$ and hot-band transitions but often have significantly larger uncertainties and a much increased chance of misassignment and mislabelling. Indeed, the hot emission spectra of 12HaLiBeb [138] remain substantially unassigned.

Some of the papers on ammonia spectra [32–34,36, 38,39,51,55,57,66,71,78,81,90,94,97,101,108,117] report only (temperature-dependent) line intensity or lineshape data or treat the theory of the ammonia spectra [70,83,110, 118,133,134,181]; therefore, they are not employed in a direct fashion in this study though they proved to be useful during the preliminary analysis of the measured transitions. Some of the papers contain unassigned transitions which were not used during the MARVEL analysis though attempts, described above, were made to add missing vibrational labels to assigned but partially labelled spectra.

Measured spectra of $^{14}NH_3$ vapor are basically a superposition of two separate spectra, that of ortho-ammonia and para-ammonia, the strongly forbidden transitions between the two nuclear-spin isomers have never been observed. Nuclear quadrupole moments, $Q$, characterize the deviation of the electrical charge distribution of an atomic nucleus from perfect spherical symmetry. $Q(^{14}N)$ is much bigger than $Q(^{1}H)$. Thus, $^{14}NH_3$ energy levels experience considerable hyperfine splitting leading to a hyperfine structure (hfs) [113,123]. The hfs is not taken into account in the present study.

The information about the experimental sources of rovibrational transitions, including wavenumber range and physical conditions of the measurements, as well as the total number of measured and validated transitions of the source are given in Table 2. Comments relevant to the characterization of the sources is provided in Section 3.2.

### 3.1. Magic numbers

MARVEL results in the correct energy levels in an absolute sense for components not connected to the principal components (PC) of the SN of $^{14}NH_3$ only if the value of the lowest-energy level within a higher-energy component, zero by definition, is shifted to the correct transition energy. It is rather difficult to connect any floating components to the two principal components. Due to the limited amount of pure rotation data for $^{14}NH_3$, the experimental SN contains 154 FCs, composed of 462 transitions. To maintain the experimental character of the MARVEL energy levels, no attempt was made to connect the FCs to the PCs using information from either EHs or first-principles computations.

Since the energy separation between ortho and para states is not measured experimentally, it is necessary to fix it for the lowest ortho and para levels using what we call a magic number. This was done by setting the energy of the $(000^00^0)$ [11] state to 16.172993 $cm^{-1}$ resulting from an EH fit [52], with an assumed zero uncertainty.

### 3.2. Comments on the data sources

(IIa) 98BeUrWi [91]: Rotation–vibration transitions in the $\nu_2$ band.

(IIb) 81UrSpPaKa [45]: The lines measured include a few $\Delta k = \pm 3$ "perturbation allowed" transitions.

(IIc) 88TaEnHi [69]: Reports $Q$-branch ($\Delta J = 0, J = 4-10$) $\Delta k = \pm 1 \leftarrow \mp 2$ rotational "perturbation-allowed" $s \leftarrow s$ and $a \leftarrow a$ transitions in the submillimeter-wave region (around 330 GHz).

(IId) 10YuPeDrSu [129]: Employed numerous spectroscopic techniques to study high $J$ transitions of the ground and the $\nu_2$ states. Measurements were carried out using a frequency multiplied submillimeter spectrometer at the Jet Propulsion Laboratory (JPL), a tunable far-infrared spectrometer at the University of Toyama, and a high-resolution Bruker IFS 125 Fourier transform spectrometer (FTS) at the synchrotron facility SOLEIL. Highly excited ammonia was created using radiofrequency and dc discharges, which allowed assignments of transitions with $J$ up to 35. This source contains 222 $\Delta k = 3$ transitions assigned for the first time.

(IIe) 99KlBrTaKo [95]: The $A/V$ values concerning the transitions originally assigned in this source are 2223/2205.

(IIf) 86HeBiBa [58]: This source contains a substantial number of unassigned lines.

(IIg) 83UrPaKaYa [50]: Nine calculated lines removed prior to the MARVEL analysis.

(IIh) 11ZoShOvPo [135]: Presents a partial assignment of the emission spectra due to 12HaLiBeb [138]. 12HaLiBeb recorded ammonia emissions at a range of temperatures comprising 100 °C intervals between 300 and 1300 °C plus 1370 °C. Two regions are covered: 740–1690 $cm^{-1}$ (region A) and 1080–2200 $cm^{-1}$ (region B). All spectra were recorded at a resolution of 0.01 $cm^{-1}$ and were generated from 240 and 80 scans for regions A and B, respectively. The overall accuracy of the line positions after calibration is about $\pm 0.002$ $cm^{-1}$. An unassigned experimental linelist based on these spectra was provided by 12HaLiBea [137].

(IIi) 78Nereson [35]: Contains 50 measured lines in the 10.6 μm region but only 27 of them could be assigned.

(IIj) 00UrHeKhFi [98]: High-accuracy vibration–rotation–inversion frequencies.

(IIk) 11LeTrDaBo [136]: A high-accuracy determination of a single line complete with full hyperfine structure as part of a campaign to get a more accurate determination of the Boltzmann constant, $k_B$.

(IIl) 98FiKhRuLe [92]: Double-resonance sub-Doppler study of the allowed and $\Delta k = -3$ forbidden $Q(3,3)$ transitions which have $v=2$. There is only one measured transition in this source, all others are calculated ones.

(IIm) 11GuJeMoPe [132]: Hot ammonia spectra.

(IIn) 84UrCuNaPa [52]: Transitions within the $\nu_4$ state, including "forbidden" $\Delta k = \pm 2$ ones. This source contains low-energy transitions corresponding to an effective Hamiltonian and these transitions have been used successfully at an early stage of the study to ensure the completeness of the pure rotational energy levels.

(IIo) 13DoHiYuTe[142]: The database provided in this paper contains 40 227 transitions. Only the 2103 newly assigned experimental transitions were utilized during the present analysis.

(IIp) 01CoTaKlBr [99]: The initial uncertainty employed during the MARVEL analysis is $\pm 0.002$ $cm^{-1}$.

**Table 2**
Data sources and their characteristics for $^{14}NH_3$. See Section 3.2 for comments.[a]

| Tag | Range ($cm^{-1}$) | Trans. | Physical conditions | | | | Comments |
|---|---|---|---|---|---|---|---|
| | | *A*/*V* | *T* (K) | *p* (hPa) | Rec. | *L* (m) | |
| 75PoKa [31] | 0.24–1.3 | 119 /119 | 373 | 0.004–0.01 | | | |
| 74CoPo [30] | 0.69–2.0 | 50/50 | RT | | SMW | | |
| 80Cohen [41] | 2.1–4.1 | 18/18 | RT | | SMW | | |
| 82SaHaAmSh [46] | 2.3–5.9 | 12/12 | 373 | 0.04 | LSS,SMW | 0.3/3.5 | |
| 92SaEnHiPo [76] | 2.4–1859.7 | 808/805 | RT | 0.04 | SMW,FTS | 3.5/2.0 | |
| 98BeUrWi [91] | 4.7–25.7 | 5/5 | RT | 0.004 | | 3.9 | (IIa) |
| 81UrSpPaKa [45] | 4.7–969.0 | 299/299 | RT | 1.05 | SMW | | (IIb) |
| 84PoMa [51] | 10–1250.2 | 534/532 | RT,296 | 0.07–3.3 | FTS | 0.2,0.5 | |
| 88TaEnHi [69] | 10.7–11.1 | 14/14 | RT | 0.07 | LMDR | 3.5 | (IIc) |
| 10YuPeDrSu [129] | 13.3–832.7 | 2166/1782 | | | THz | | (IId) |
| 06ChPePiMa [182] | 15.6–46.4 | 30/30 | 77,300 | 0.07–0.27 | | | |
| 71HeDeGo [29] | 19.9–19.9 | 1/1 | RT | | SMW | 0.3 | |
| 94BrPe [81] | 39.0–219,3331–3415 | 174/174 | | | | | |
| 96KrTrBoBa [86] | 40.5–40.5 | 1/1 | RT | | SMW,THz | | |
| 11DrYuPeGu [130] | 84.0–89.0 | 5/5 | 18 | 0.07–0.67 | SMW,THz | 0.06 | |
| 99KlBrTaKo [95] | 363–3634 | 2223/2209 | 296 | 0.05–0.31 | FTS | 0.1–73 | (IIe) |
| 86UrCuMaNa [62] | 511–1351 | 599/576 | RT | 0.01,0.2 | FTS | 192 | |
| 86HeBiBa [58] | 620–739 | 184/184 | | | | | (IIf) |
| 80UrSpPaMc [42] | 678–2014 | 333/333 | RT | 0.27–13.3 | IR,GRS | | |
| 83UrPaKaYa [50] | 709–1159 | 640/639 | RT | 1 | FTS,DFLS | 0.6 | (IIg) |
| 99FaYa [94] | 771–1179 | 126/126 | | | | | |
| 86SaScMaPo [60] | 772–1157 | 138/138 | | | | | |
| 11ZoShOvPo [135] | 780–2029 | 6119/5897 | 573–1593 | 0.001–0.66 | FTS,EMS | 1.2 | (IIh) |
| 85BrTo [54] | 814–1122 | 81/81 | RT | 0.001 | FTS | 2.4–193 | |
| 84Weber [53] | 853–1880 | 176/174 | RT | 0.013 | | 0.25 | |
| 94ChChCh [82] | 929–955 | 49/49 | | | | | |
| 81SaMiWo [43] | 933–1085 | 32/32 | | | | | |
| 78Nereson [35] | 943–956 | 27/27 | | | | | (IIi) |
| 00UrHeKhFi [98] | 948–952 | 2/2 | RT | 0.0001–0.0007 | IR-IR,SDST | 2.0 | (IIj) |
| 79HiJeFa [38] | 949–949 | 1/1 | RT | 0.13 | DFLS | 0.3 | |
| 11LeTrDaBo [136] | 966-966 | 1/1 | 273.15 | | | | (IIk) |
| 98FiKhRuLe [92] | 967–967 | 1/1 | RT | 0.004 | | 1.4 | (IIl) |
| 11GuJeMoPe [132] | 1126–1171 | 22/22 | 253–296 | 1.6–20 | FTS | | (IIm) |
| 84UrCuNaPa [52] | 1168–2127 | 951/941 | RT | 0.01,0.2 | FTS | 1.5 | (IIn) |
| 13DoHiYuTe[142] | 1170–5170 | 2103/2103 | | | | | (IIo) |
| 01CoTaKlBr [99] | 1202–2749 | 1323/1321 | 295–300 | 0.3–3.3 | FTS | 0.25–433 | (IIp) |
| 00CoKlTaBr [96] | 1333–3454 | 1202/1198 | 295–300 | 0.3–1.3 | IR-IR | 0.04–433 | (IIq) |
| 95KlTaBr [84] | 2087–3115 | 2207/2117 | 294–298 | 0.06–0.9 | FTS | 1.5 | |
| 89GuAbTuRa [71] | 3023–3675 | 1375/1375 | | | | | |
| 85AnFiFrIl [183] | 3135–3620 | 624/610 | 297 | 6.7–26.7 | DFLS | 1.5 | (IIr) |
| 85UrMiRa [56] | 3148–4504 | 481/479 | | | | | |
| 93PiDa [79] | 3331–3415 | 100/100 | 297 | 6.7–26.7 | DFLS | 0.58 | (IIs) |
| 14DiMiQuSc [147] | 3355–3355 | 1/1 | | | | | (IIt) |
| 89UrTuRaGu [72] | 3970–4648 | 892/890 | | | | | |
| 14CeHoVeCa [146] | 4275–4340 | 235/230 | | | | | |
| 96BrMa [85] | 4791–5293 | 638/638 | RT,cold | 0.0013 | FTS | 0.25–25.0 | (IIu) |
| 12SuBrHuSc [140] | 6347–6974 | 1089/1058 | 185–296 | 0.1–2.7 | FTS | 0.25–24.4 | (IIv) |
| 93LuHeNi [77] | 6405–6881 | 380/332 | 293–294 | 2.1,1.3 | FTS | 0.2–2.4 | (IIw) |
| 14FoGoHeSo [148] | 6410–6764 | 144/144 | 14 | 830/0.15 | CRDS,CEAS | max.700 | (IIx) |
| 07LiLeXu [115] | 6421–6678 | 104/104 | | | | | (IIy) |
| 08LeLiXu [119] | 6440–6832 | 233/194 | RT | 0.4 | VISTA | 2.8 | (IIz) |
| 10PeHa [128] | 6460–6541 | 14/12 | | | | | |
| 04XuLiYaTr [108] | 6466 | 1/1 | | | | | |
| 99BePeMe [93] | 6540–6625 | 22/22 | 10,30 | 0.003 | CEAS | | (IIaa) |
| 86CoLe [57] | 15259–15553 | 323/321 | 200,295 | | MODR | | (IIbb) |

[a] The tags listed are used to identify experimental data sources throughout this paper. The range given represents the range corresponding to validated wavenumber entries within the MARVEL input file and not the range covered by the relevant experiment. Uncertainties of the individual lines can be obtained from the Supporting Information. Trans.=transitions, with *A*=number of assigned transitions in the original data source, *V*=number of transitions validated in this study. *T*=temperature (K), given explicitly when available from the original publication, with RT=room temperature. *p*=pressure (hPa). Rec.=experimental technique used for the recording of the spectrum, with CARS=coherent anti-Stokes Raman spectroscopy, CEAS=cavity enhanced absorption spectroscopy, CRDS=cavity ringdown spectroscopy, DFLS=difference frequency laser spectroscopy, EMS=emission spectroscopy, FMSS=frequency-multiplied sub-millimeter spectroscopy, FTS=Fourier-transform spectroscopy, ICLAS=intracavity laser absorption spectroscopy, LD=Lamb dip, LMDR=laser-microwave double resonance, MMW=millimeterwave spectroscopy, MODR=microwave double resonance spectroscopy, MRE=multiresonance experiment, NR=not relevant, SMW=submillimeter-microwave spectrometer, THz=terahertz spectrometer, TuFIR=tunable far infrared, and VISTA=vibrational isotopic shift technique spectroscopy.

(IIq) 00CoKlTaBr [96]: Terahertz spectroscopy in the $v_2=1$ state. The $A/V$ values concerning the transitions originally assigned are 1180/1176.

(IIr) 85AnFiFrIl [183]: Besides the transitions employed in this study, this source contains 60 Raman lines that are not included in the MARVEL database.

(IIs) 93PiDa [79]: Uncertainty used is 0.001 $cm^{-1}$.

(IIt) 14DiMiQuSc [147]: Molecular beam study of a single line using two photon infrared-laser induced population transfer; the high resolution study resolves the hyperfine structure.

(IIu) 96BrMa [85]: This is a distinct source covering the region 4790–5295 $cm^{-1}$ within HITRAN [184], from where most of the lines were taken. As pointed out in 13DoHiYuTe [142], versions earlier than 2012 of HITRAN [185,186] contained a mistake which made almost all of the 96BrMa transitions strongly forbidden. This paper suggests that 89CoLe [70] should be recalibrated by $+0.004$ $cm^{-1}$. No recalibration was attempted during the MARVEL analysis.

(IIv) 12SuBrHuSc [140]: High-resolution spectra recorded at an unapodized resolution of about 0.0111 from 3000 to 7500 $cm^{-1}$ with a signal to noise ratio of nearly 1000:1, using the McMath-Pierce FTS located at Kitt Peak National Observatory. Residual $H_2{}^{16}O$ features inside the FTS were used for frequency calibration. The accuracy of the measured lines goes from 0.0001 to 0.003 $cm^{-1}$, the latter for badly blended features. This source contains a substantial number of unassigned lines.

(IIw) 93LuHeNi [77]: Contains a total of 1710 observed lines from spectra of the 1.5 μm region recorded using a FTS. Assignments, performed through the ground-state combination difference (GSCD) technique, are reported for 283 lines in the strong $\nu_1+\nu_3$ combination band and for 98 in the weak $2\nu_3$ overtone band. Consequently, numerous lines remained unassigned in the spectra. There are indications from more recent measurements [101,125] that a small ($\approx 0.002$ $cm^{-1}$) recalibration of 93LuHeNi data may be required. However, the more recent measurements are for only relatively few lines and thus no recalibration [166] was attempted during the MARVEL analysis.

(IIx) 14FoGoHeSo [148]: Jet-cooled spectra of ammonia, the rotational temperature is around 14 K and 17 K in the CRDS and CEAS experiments, respectively. The paper strictly focuses on rotational issues and vibrational labels are provided in this work. We were able to give vibrational labels to 144 of the 265 measured lines presented.

(IIy) 07LiLeXu [115]: This paper reports lines from two experiments: most lines were recorded using an external cavity tunable diode laser (ECTDL) spectrometer but a set of 15 lines were recorded using an FTS under unspecified conditions, these lines are cited as N. Ibrahim, J. Orphal, P. Chelin, C.E. Fellows (2005). We note that 08LeOrRuHe [120] reported an unassigned FTS spectrum in this region, alongside an unassigned CDEAS spectrum recorded at higher frequencies, but the line positions do not correspond with those reported by 07LiLeXu.

(IIz) 08LeLiXu [119]: ECTDL spectra recorded from 6400 to 6808 $cm^{-1}$. This paper uses VISTA, a vibrational isotopic shift technique, for assignment, for classifying spectral lines into their respective absorption bands from their fingerprint isotopic shifts.

(IIaa) 99BePeMe [93]: The significantly simplified spectrum, containing only transitions starting from $J''=0,1,2$, of two perpendicular bands, $\nu_1+\nu_3$ and $\nu_1+2\nu_4$, of rotationally cold (temperature between 10 K and 30 K) ammonia was recorded using a diode laser. No band heads have been observed due to their low intensity. Eighteen $\nu_1+\nu_3$ and nine $\nu_1+2\nu_4$ ($l_4=2$) transitions were reported. Lines in this spectrum are calibrated to lines given by 93LuHeNi [77]; since no uncertainty is given the uncertainty given by 93LuHeNi, $\pm 0.001$ $cm^{-1}$ was assumed.

(IIbb) 86CoLe [57]: This paper reports spectra recorded using both microwave-detected microwave-optical double resonance spectra and of photoacoustic absorption spectra which probed N–H 5 and 6 quanta overtones. Vibrational state labels, given here as described in Section 2.4, must be regarded as arbitrary.

## 4. MARVEL energy levels

### 4.1. The SN of $^{14}NH_3$

Discussion of the experimental-type MARVEL energy levels cannot be complete without first discussing the spectroscopic network resulting in the MARVEL energy levels.

The rotational–vibrational transitions characterizing one-photon (absorption or emission) experiments form a spectroscopic network (SN) [159,160,172]. SNs are large, finite, weighted, rooted graphs, where the vertices are discrete energy levels (with associated uncertainties), the edges are transitions (with measured uncertainties), and in a simple picture the weights are provided by the transition intensities. The root of the graph is the lowest energy level. According to the quantum mechanical selection rules, the transitions of $^{14}NH_3$ generate two principal components (PCs). The root of the para component is the [$J$ $K$]=[0 0] energy level of the ground vibrational state, while the root of the ortho component is the [$J$ $K$]= [1 1] level of the same VBO.

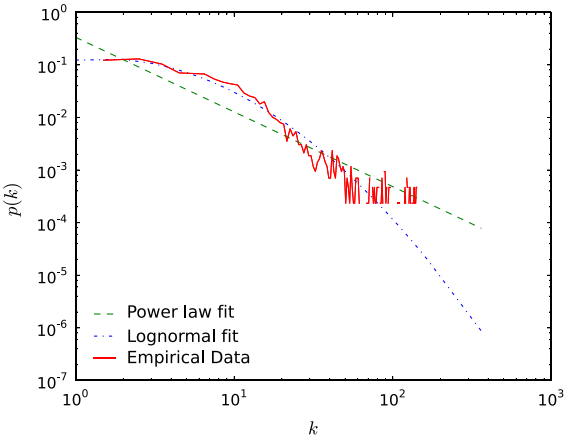


**Fig. 1.** Size-frequency distribution of the experimental spectroscopic network of $^{14}NH_3$.

**Table 3**
Vibrational band origins (VBOs) for $^{14}NH_3$, with standard abbreviated (SA) and detailed normal-mode ($v_1$ $v_2$ $v_3$ $v_4$ $L_3$ $L_4$ $L$) labels, vibrational symmetries ($\Gamma_v$), MARVEL uncertainties (Unc.), and the number of validated rotational–vibrational levels (RL) associated with the vibrational levels present in the MARVEL database.[a]

| SA | $v_1$ $v_2$ $v_3$ $v_4$ $L_3$ $L_4$ $L$ | $\Gamma_v$ | VBO/cm$^{-1}$ | Unc.[a] | RL |
|---|---|---|---|---|---|
| ZPVE $\equiv 0^+$ | 0 0 0 0 0 0 0 | $A_1'$ | 0.000000[b] | 994 | 359 |
| $0^-$ | 0 0 0 0 0 0 0 | $A_2''$ | 0.794368 | 697 | 355 |
| $\nu_2^+$ | 0 1 0 0 0 0 0 | $A_1'$ | [932.4] | | 306 |
| $\nu_2^-$ | 0 1 0 0 0 0 0 | $A_2''$ | 968.122894 | 497 | 310 |
| $2\nu_2^+$ | 0 2 0 0 0 0 0 | $A_1'$ | [1597.5] | | 172 |
| $\nu_4^+$ | 0 0 0 1 0 1 1 | $E'$ | 1626.274636 | 1544 | 295 |
| $\nu_4^-$ | 0 0 0 1 0 1 1 | $E''$ | 1627.372362 | 2168 | 300 |
| $2\nu_2^-$ | 0 2 0 0 0 0 0 | $A_2''$ | 1882.178422 | 1152 | 225 |
| $3\nu_2^+$ | 0 3 0 0 0 0 0 | $A_1'$ | [2384.2] | | 98 |
| $(\nu_2+\nu_4)^+$ | 0 1 0 1 0 1 1 | $E'$ | 2540.523012 | 1411 | 162 |
| $(\nu_2+\nu_4)^-$ | 0 1 0 1 0 1 1 | $E''$ | 2586.126091 | 1980 | 164 |
| $3\nu_2^-$ | 0 3 0 0 0 0 0 | $A_2''$ | 2895.522916 | 1411 | 87 |
| ⋮ | 1 state missing at 3189($E'$) | | | | |
| $2\nu_4^{0,+}$ | 0 0 0 2 0 0 0 | $A_1'$ | [3216.0] | | 61 |
| $2\nu_4^{0,-}$ | 0 0 0 2 0 0 0 | $A_2''$ | 3217.588264 | 1782 | 48 |
| $2\nu_4^{2,+}$ | 0 0 0 2 0 2 2 | $E'$ | 3240.162903 | 3086 | 117 |
| $2\nu_4^{2,-}$ | 0 0 0 2 0 2 2 | $E''$ | 3241.598311 | 1782 | 106 |
| $\nu_1^+$ | 1 0 0 0 0 0 0 | $A_1'$ | [3336.1] | | 62 |
| $\nu_1^-$ | 1 0 0 0 0 0 0 | $A_2''$ | 3337.097887 | 3651 | 62 |
| $\nu_3^+$ | 0 0 1 0 1 0 1 | $E'$ | 3443.628071 | 968 | 125 |
| $\nu_3^-$ | 0 0 1 0 1 0 1 | $E''$ | 3443.987642 | 968 | 131 |
| $4\nu_2^+$ | 0 4 0 0 0 0 0 | $A_1'$ | [3462.5] | | 20 |
| $(2\nu_2+\nu_4)^-$ | 0 2 0 1 0 1 1 | $E''$ | [3502.1] | | 10 |
| ⋮ | 2 states missing at 4007($E'$) & 4062($A_2''$) | | | | |
| $(\nu_2+2\nu_4^0)^+$ | 0 1 0 2 0 0 0 | $A_1'$ | [4115.6] | | 24 |
| $(\nu_2+2\nu_4^2)^+$ | 0 1 0 2 0 2 2 | $E'$ | [4135.9] | | 22 |
| $(\nu_2+2\nu_4^0)^-$ | 0 1 0 2 0 0 0 | $A_2''$ | [4173.3] | | 12 |
| $(\nu_2+2\nu_4^2)^-$ | 0 1 0 2 0 2 2 | $E''$ | [4193.1] | | 22 |
| $(\nu_1+\nu_2)^+$ | 1 1 0 0 0 0 0 | $A_1'$ | [4294.5] | | 69 |
| $(\nu_1+\nu_2)^-$ | 1 1 0 0 0 0 0 | $A_2''$ | 4320.031622 | 2080 | 70 |
| $(\nu_2+\nu_3)^+$ | 0 1 1 0 1 0 1 | $E'$ | 4416.915038 | 1000 | 109 |
| $(\nu_2+\nu_3)^-$ | 0 1 1 0 1 0 1 | $E''$ | 4435.446463 | 2000 | 112 |
| ⋮ | 2 states missing at 4530($E''$)&4695($A_1'$) | | | | |
| $(2\nu_2+2\nu_4^0)^+$ | 0 2 0 2 0 0 0 | $A_1'$ | [4754.3] | | 1 |
| ⋮ | 2 states missing at 4773($E'$)&4800($E'$) | | | | |
| $3\nu_4^{1,-}$ | 0 0 0 3 0 1 1 | $E''$ | [4802.4] | | 1 |
| ⋮ | 4 states missing (4842–4845) | | | | |
| $(\nu_1+\nu_4)^+$ | 1 00 1 0 1 1 | $E'$ | 4955.756078 | 1000 | 100 |
| $(\nu_1+\nu_4)^-$ | 1 0 0 1 0 1 1 | $E''$ | [4956.9] | | 23 |
| $(\nu_1+2\nu_2)^+$ | 1 2 0 0 0 0 0 | $A_1'$ | [5002.9] | | 1 |
| $(\nu_3+\nu_4)^+$ | 0 0 1 1 1 1 0 | $A_2''$ | [5051.4] | | 30 |
| $(\nu_3+\nu_4)^-$ | 0 0 1 1 1 1 0 | $A_1''$ | [5052.1] | | 23 |
| ⋮ | 4 states missing (5052–5070) | | | | |
| $(2\nu_2+2\nu_4^0)^0$ | 0 2 0 2 0 0 0 | $A_2''$ | [5092.6] | | 1 |
| ⋮ | 1 state missing at 5103($E'$) | | | | |
| $(2\nu_2+2\nu_4^2)^-$ | 0 2 0 2 0 2 2 | $E''$ | [5112.8] | | 2 |
| $(2\nu_2+\nu_3)^+$ | 0 2 1 0 1 0 1 | $E'$ | [5146.3] | | 16 |
| $(2\nu_2+\nu_3)^-$ | 0 2 1 0 1 0 1 | $E''$ | [5352.8] | | 11 |
| ⋮ | 25 states missing (5235–6231) | | | | |
| $(2\nu_2+3\nu_4^1)^+$ | 0 2 0 3 0 1 1 | $E'$ | [6310.3] | | 3 |
| ⋮ | 10 states missing | | | | |
| $2\nu_1^+$ | 2 0 0 0 0 0 0 | $A_1'$ | [6514.1] | | 1 |
| ⋮ | 1 state missing | | | | |
| $(\nu_1+2\nu_4^2)^+$ | 1 0 0 2 0 2 2 | $E'$ | 6556.421597 | 1988 | 38 |
| $(\nu_1+2\nu_4^2)^-$ | 1 0 0 2 0 2 2 | $E''$ | 6557.930442 | 5185 | 40 |
| ⋮ | 3 states missing | | | | |
| $(\nu_1+\nu_3)^+$ | 1 0 1 0 1 0 1 | $E'$ | 6608.821870 | 1988 | 75 |
| $(\nu_1+\nu_3)^-$ | 1 0 1 0 1 0 1 | $E''$ | 6609.753328 | 2478 | 77 |
| $(\nu_1+2\nu_4^0)^+$ | 1 0 0 2 0 0 0 | $A_1'$ | [6648.2] | | 1 |
| $(\nu_1+2\nu_4^0)^-$ | 1 0 0 2 0 0 0 | $A_2''$ | [6649.8] | | 1 |
| $(\nu_3+2\nu_4^0)^+$ | 0 0 1 2 1 0 0 | $A_2'$ | [6651.4] | | 3 |

**Table 3** (*continued*)

| SA | $v_1$ $v_2$ $v_3$ $v_4$ $L_3$ $L_4$ $L$ | $\Gamma_v$ | VBO/cm$^{-1}$ | Unc.[a] | RL |
|---|---|---|---|---|---|
| $(\nu_3+2\nu_4^0)^-$ | 0 0 1 2 1 0 0 | $A_1''$ | [6652.6] | | 3 |
| ⋮ | 2 states missing | | | | |
| $(\nu_3+2\nu_4^2)^+$ | 0 0 1 2 1 2 1 | $E'$ | 6677.431678 | 1990 | 59 |
| $(\nu_3+2\nu_4^2)^-$ | 0 0 1 2 1 2 1 | $E''$ | 6678.310343 | 1990 | 60 |
| $(\nu_2+3\nu_4^1)^-$ | 0 2 0 3 0 1 1 | $E''$ | 6678.929943 | 2000 | 3 |
| ⋮ | 8 states missing | | | | |
| $2\nu_2+\nu_3+\nu_4$ | 0 2 1 1 1 1 0 | $A_1'$ | [6719.3] | – | 1 |
| $2\nu_3$ | 0 0 2 0 0 0 0 | $A_2''$ | [6792.0] | | 24 |
| $2\nu_3$ | 0 0 2 0 0 0 0 | $A_1'$ | [6793.1] | | 26 |
| ⋮ | 1 state missing ($E''$) | | | | |
| $2\nu_3$ | 0 0 2 0 2 0 2 | $E'$ | 6850.244878 | 5300 | 17 |
| $2\nu_3$ | 0 0 2 0 2 0 2 | $E''$ | 6850.654943 | 3900 | 18 |

[a] The VBOs are reported in the order of increasing energy. The uncertainties are given in units of $10^{-6}$ cm$^{-1}$. The approximate VBO values given in brackets are taken from Ref. [187].

[b] The value of the vibrational ground state was fixed to zero with zero uncertainty.

The size-frequency $[k-p(k)]$ distribution of the links is one of the most important properties of complex networks. As earlier studies suggested for asymmetric tops [159,160,172], the degree-distribution functions of experimental SNs of molecules show a heavy-tailed distribution, indicating that the SNs are characterized by hubs, *i.e.*, a small number of nodes with a large number of connections. Fig. 1 depicts the degree-distribution function of $^{14}NH_3$, exhibiting the expected heavy-tailed behavior. As observed before [172], it is hard to distinguish between the power-law and the log-normal distributions, *i.e.*, whether the degree distribution follows a power-law or log-normal distribution. Nevertheless, it is clear that the experimental SN of $^{14}NH_3$ contains hubs. As expected, the most important hubs are on the ground vibrational state. The three largest hubs are as follows: $[J\ K\ \Gamma_r]=[5\ 3\ A_1'']$, $[5\ 3\ A_2'']$, and $[4\ 2\ E']$ with 170, 167, and 161 links, respectively. This observation agrees with our earlier experience [160] that the rotational quantum numbers of the hubs are about $J$=4–6, which is partly due to the fact that most measurements are performed at room temperature.

### 4.2. Comparison of MARVEL and BYTe energy levels

As an independent validation of the MARVEL energy levels and their labels, systematic comparisons were performed with variational nuclear motion computations. For this comparison the so-called BYTe [134] (see Section 2.4) energy list was used.

Since neither the rotational nor the vibrational labels of the energy levels in BYTe are derived from experiments, the MARVEL and the BYTe labels are occasionally different. Therefore, only the values of energies, the exact descriptors, and the inversion symmetry were used for comparison. We used a matching cut-off of 0.5 cm$^{-1}$ between the MARVEL and BYTe energies up to 5000.0 cm$^{-1}$ and 1.0 cm$^{-1}$ above this energy. The BYTe list provides the rotational ($\Gamma_{rot}$), the vibrational ($\Gamma_{vib}$), and the total symmetry ($\Gamma_{tot}$), but only the total symmetry is exact. Therefore, (in a few cases) the rotational and vibrational symmetries of the MARVEL levels may differ from the BYTe symmetry labels. Nevertheless, each MARVEL level fulfills $\Gamma_{rot}^{MARVEL}\otimes\Gamma_{vib}^{MARVEL}=\Gamma_{tot}^{BYTe}$. As a result, each MARVEL energy level has a corresponding BYTe energy level, as far as the value of the energy level, the $J$ quantum number and the total symmetry are concerned.

### 4.3. VBOs

The MARVEL VBOs determined for $^{14}NH_3$ are given in Table 3. Despite the fact that a large number of rovibrational transitions have been measured for $^{14}NH_3$, there are only 25 VBOs, seven for ortho- and 18 for para-$^{14}NH_3$, determined for this molecule. However, it should be noted that direct determination of the VBO states of $A_1^+$ symmetry is not possible since these states cannot possess a rotationless ($J$=0) state. In fact, the coverage of VBOs is complete up to 3500 cm$^{-1}$, the first missing VBO, of $E''$ symmetry, is at 3502 cm$^{-1}$. That more para-$^{14}NH_3$ VBOs are known than ortho ones is in line with the fact that a larger number of para-$^{14}NH_3$ energy levels are known, despite that the spin-statistical weight is twice as large for the ortho levels. This is due to the selection rules governing the transitions.

The uncertainties of the VBOs are fairly substantial, usually on the order of 0.001–0.004 cm$^{-1}$. This calls for new measurements employing highly accurate new techniques, such as frequency combs, to further improve our understanding of the vibrational energy level structure of $^{14}NH_3$.

To understand some of the complexity underlying the measured spectra of $^{14}NH_3$ and the assignment procedure, we note that, based on earlier *ab initio* computations [118,133], there are up to 43 VBOs in the range 6300–7000 cm$^{-1}$ alone. As Table 3 shows, considerably less than half of these VBOs are involved in measured transitions and only a few VBOs became known based on the MARVEL analysis of all available experimental transitions.

### 4.4. Prediction of unmeasured lines

Our MARVEL procedure yields 4961 energy levels based on the analysis of 28 530 validated “networked” transitions.

However, the number of allowed transitions between the MARVEL energy levels is actually substantially more than this number. Fig. 2 shows an analysis of this for spectra at 296 K. It compares the spectrum arising from the transitions analyzed with those obtained by including allowed transitions between MARVEL levels and the full spectrum predicted by BYTe. It can be seen that use of MARVEL predicted transitions helps to give an ammonia spectrum with a much more complete coverage. In particular, MARVEL predicts a number of transitions in the range 5300–6340 $cm^{-1}$ where currently there are no reported observations; these transitions are largely associated with hot bands for which lower and upper states are determined experimentally. Any overtone or combination bands arising from the ground vibrational state are still missing and it can be seen that the BYTe predictions contain stronger lines in this region than those identified using MARVEL energies. Finally we note that while line intensities predicted by BYTe are excellent for some low-lying bands [142], they do show differences when compared with the observations [188] which, in general, increase in frequency.

Fig. 2 also shows the spectrum of ammonia currently available from the HITRAN 2012 database [184]. This latest edition of HITRAN contains 45 302 lines for $^{14}NH_3$ (and 1090 for $^{15}NH_3$). As summarized in Table 2 of Ref. [142], in the 2008 edition of HITRAN there were 27 994 $^{14}NH_3$ transitions coming from nine sources. We note that not all the lines included in HITRAN 2012 are the result of actual experimental measurement. Indeed, the 2012 update to HITRAN contains transitions in several bands predicted by 13DoHiYuTe [142] on the basis of empirical energy levels and first principles (BYTe) transition intensities. We suggest that a significantly better coverage could be obtained by extending this analysis using our new set of energy levels. A list of predicted lines synthesized from MARVEL energy levels and BYTe intensities is given in the Supporting Information.

## 5. Summary and conclusions

The complexity of high-resolution $^{14}NH_3$ spectra, emphasized already by Herzberg [189], hinders significantly the application of standard tools of molecular spectroscopy, including effective Hamiltonians, for their analysis. Advancements in the fourth age of quantum chemistry [152] make possible the extensive use of sophisticated variational nuclear motion techniques which help to decipher even complex spectral features and can be used to correct problems existing databases, like HITRAN, used to have about the linelist of $^{14}NH_3$. The repertoire of useful novel tools to study spectra of $^{14}NH_3$ has been extended in this study with the MARVEL procedure, standing for Measured Active Rotational–Vibrational Energy Levels, allowing the empirical investigation and self-consistent verification of all measured and labelled transitions and yielding experimental energy levels with self-consistent uncertainties.

As part of the MARVEL analysis, we collected 29 450 measured transitions from 56 sources which, after careful checking and labelling, underwent a MARVEL analysis and resulted in 1724 and 3237 energy levels for ortho- and para-$^{14}NH_3$, respectively. This set of experimental energy levels should prove highly useful in all future analysis of experimental spectra of $^{14}NH_3$. Based on MARVEL energy levels and BYTe intensities, a linelist has been generated, and deposited in the Supporting Information to this paper.

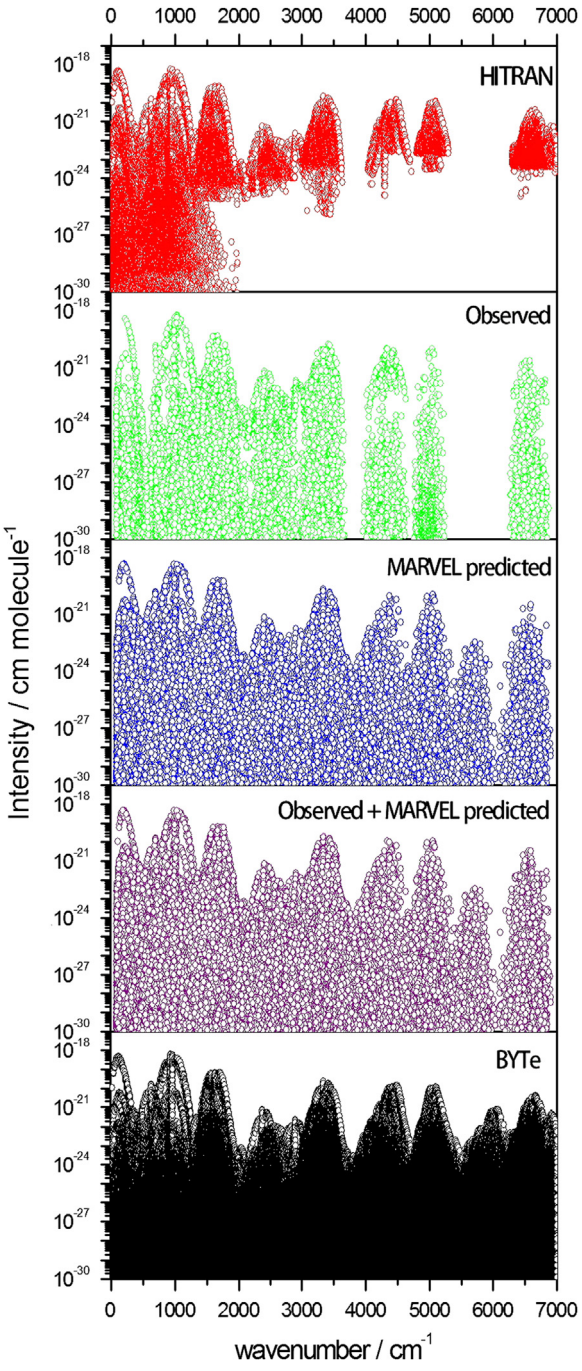


**Fig. 2.** Comparison of spectra at 296 K for one-photon absorption transitions of $^{14}NH_3$ up to 7000 $cm^{-1}$. Top panel – lines present in the HITRAN [184] database; second panel – observed transitions present in MARVEL; third panel – MARVEL predicted transitions, omitting lines which have already been observed; fourth panel – sum of the observed and MARVEL predicted transitions; and bottom panel – all lines predicted by variational computations (BYTe [176]). Except for the top panel, all intensities come from BYTe.

This linelist and the associated comparison of "observed" and "MARVEL predicted" spectra prove (see Fig. 2) how much more extensive is the information content of measured spectra if they are analyzed together, as done in MARVEL.

## Acknowledgment

We thank Drs. Stephen Coy and Isabelle Kleiner for providing copies of the supplementary material from their work, and Dr. Linda Brown for providing helpful information. This work has received partial support from the European Research Council under Advanced Investigator Project 267219, the Scientific Research Fund of Hungary (Grant OTKA NK83583), and an ERA-Chemistry grant.

## Appendix A. Supplementary data

Supplementary data associated with this paper can be found in the online version at http://dx.doi.org/10.1016/j.jqsrt.2015.03.034.

## References

[1] Almenningen A, Bastiansen O. The use of the electron diffraction sector method for location of hydrogen in gas molecules. Acta Chem Scand 1955;9:815–20.
[2] Benedict WS, Plyler EK. Vibration-rotation bands of ammonia. II. The molecular dimensions and harmonic frequencies of ammonia and deuterated ammonia. Can J Phys 1957;35:1235–41.
[3] Kuchitsu K, Guillory JP, Bartell LS. Electron-diffraction study of ammonia and deuteroammonia. J Chem Phys 1963;49:2488–93.
[4] Tavard C, Roualt M, Roux M, Cornille M. Calculation of X-ray and electron intensities scattered by the $NH_3$ and $H_2O$ molecules. J Chem Phys 1963;39:2390–1.
[5] Bastiansen O, Beagley B. A comparison of the molecular structures of ammonia and deuteroammonia as determined by electron diffraction. Acta Chem Scand 1964;18:2077–80.
[6] Morino Y, Kuchitsu K, Yamamoto S. The anharmonic constants and average structure of ammonia. Spectrochim Acta A 1968;24:335–52.
[7] Bunker PR, Kraemer WP, Špirko V. An *ab initio* investigation of the potential function and rotation–vibration energies of $NH_3$. Can J Phys 1984;62:1801–5.
[8] Špirko V, Kraemer WP. Anharmonic potential function and effective geometries for the $NH_3$ molecule. J Mol Spectrosc 1989;133:331–44.
[9] Demaison J, Margulés L, Boggs JE. The equilibrium N–H bond length. Chem Phys 2000;260:65–81.
[10] Szabó I, Fábri C, Czakó G, Mátyus E, Császár AG. Temperature-dependent, effective structures of the $^{14}NH_3$ and $^{14}ND_3$ molecules. J Phys Chem A 2012;116:4356–62.
[11] Barker EF. The molecular spectrum of ammonia. II. The double band at 10 μ. Phys Rev 1929;33:684–91.
[12] Badger RM, Cartwright CH. The pure rotation spectrum of ammonia. Phys Rev 1929;33:692–700.
[13] Dennison DM, Hardy JD. The parallel type absorption bands of ammonia. Phys Rev 1932;39:938–47.
[14] Fermi E. Sulle bande di oscillazione e rotazione dell'ammoniaca. Nuovo Cimento 1932;9:277–83.
[15] Unger HJ. Infrared absorption bands of ammonia. Phys Rev 1933;43:123–8.
[16] Sheng H-Y, Barker EF, Dennison DM. Further resolution of two parallel bands of ammonia and the interaction between vibration and rotation. Phys Rev 1941;60:786–94.
[17] Gordy W, Kessler M. Microwave spectra: the hyperfine structure of ammonia. Phys Rev 1947;71:640.
[18] Nielsen HH, Dennison DM. Anomalous values of certain of the fine structure lines in the ammonia microwave spectrum. Phys Rev 1947;72:1101–8.
[19] Hauser RL, Oetjen RA. The infrared spectra of HCl, DCl, HBr, and $NH_3$ in the region 40 to 140 microns. J Chem Phys 1953;21:1340–3.
[20] Gordon JP, Zeiger HJ, Townes CH. Molecular microwave oscillator and new hyperfine structure in the microwave spectrum of $NH_3$. Phys Rev 1954;95:282–4.
[21] Gunther-Mohr GR, White RL, Schawlow AL, Good WE, Coles DK. Hyperfine structure in the spectrum of $^{14}NH_3$. I. Experimental results. Phys Rev 1954;94:1184–91.
[22] Gunther-Mohr GR, Townes CH, van Vleck JH. Hyperfine structure in the spectrum of $^{14}NH_3$. II. Theoretical discussion. Phys Rev 1954;94:1191–203.
[23] Benedict WS, Plyler EK, Tidwell ED. Vibration-rotation bands of ammonia. III. The region 3.2–4.3 microns. J Chem Phys 1958;29:829–45.
[24] Garing JS, Nielsen HH. *l*-type doubling in $NH_3$. Proc Natl Acad Sci US 1958;44:467–72.
[25] Tsuboi M, Shimanouchi T, Mizushima S. Analysis of *P*- and *R*-branches of the 950 $cm^{-1}$ band of $^{14}NH_3$. Spectrochim Acta 1958;13:80–92.
[26] Mould HM, Price WC, Wilkinson GR. A high-resolution study and analysis of the $\nu_2$ $NH_3$ vibration–rotation band. Spectrochim Acta 1959;15:313–30.
[27] Kukolich SG. Measurement of ammonia hyperfine structure with a two-cavity maser. Phys Rev 1967;156:83–92.
[28] Kukolich SG, Wofsy SC. $^{14}NH_3$ hyperfine structure and quadrupole coupling. J Chem Phys 1970;52:5477–81.
[29] Helminger P, de Lucia FC, Gordy W. Rotational spectra of $NH_3$ and $ND_3$ in the 0.5-mm wavelength region. J Mol Spectrosc 1971;39:94–7.
[30] Cohen EA, Poynter RL. The microwave spectrum of $^{14}NH_3$ in the $v=000011$ state. J Mol Spectrosc 1974;53:131–9.
[31] Poynter RL, Kakar RK. The microwave frequencies, line parameters, and spectral constants for $^{14}NH_3$. Astrophys J Suppl Ser 1975;29:87–96.
[32] Bischel WK, Kelly PJ, Rhodes CK. High-resolution Doppler-free two-photon spectroscopic studies of molecules. II. The $\nu_2$ bands of $^{14}NH_3$. Phys Rev A 1976;13:1829–41.
[33] Freund SM, Oka T. Infrared-microwave two-photon spectroscopy: the $\nu_2$ band of $NH_3$. Phys Rev A 1976;13:2178–90.
[34] Kostiuk T, Mumma MJ, Hillman JJ, Buhl D, Brown LW, Faris JL, et al. $NH_3$ spectral line measurements on Earth and Jupiter using a 10 μm superheterodyne receiver. Infrared Phys 1977;17:431–9.
[35] Nereson N. Diode laser measurements of $NH_3$ absorption lines around 10.6 μm. J Mol Spectrosc 1978;69:489–93.
[36] Sattler JP, Ritter KJ. Diode laser spectra of $NH_3$ in the 9.5-μm region. J Mol Spectrosc 1978;69:486–8.
[37] Young LDG, Young AT. An improved fit to the inversion spectrum of $^{14}NH_3$. J Quant Spectrosc Radiat Transf 1978;20:533–7.
[38] Hillman JJ, Jennings DE, Faris JL. Diode laser-$CO_2$ laser heterodyne spectrometer: measurement of $2sQ(1,1)$ in $2\nu_2-\nu_2$ of $NH_3$. Appl Opt 1979;18:1808–11.
[39] Takami M, Jones H, Oka T. Transition dipole moments of $NH_3$ in excited vibrational states determined by laser Stark spectroscopy. J Chem Phys 1979;70:3557–8.
[40] Belov SP, Gershstein LI, Krupnov AF, Maslovskij AV, Urban Š, Špirko V. Inversion and inversion-rotation spectrum of $^{14}NH_3$ in the $\nu_2$ excited state. J Mol Spectrosc 1980;84:288–304.
[41] Cohen EA. The $\nu_4$ state inversion spectra of $^{15}NH_3$ and $^{14}NH_3$. J Mol Spectrosc 1980;79:496–501.
[42] Urban Š, Špirko V, Papoušek D, McDowell RS, Nereson NG, Belov SP, et al. Coriolis and *l*-type interactions in the $\nu_2$, $2\nu_2$, and $\nu_4$ states of $^{14}NH_3$. J Mol Spectrosc 1980;79:455–95.
[43] Sattler JP, Miller LS, Worchesky TL. Diode laser heterodyne measurements on $^{14}NH_3$. J Mol Spectrosc 1981;88:347–51.
[44] Sattler JP, Worchesky TL. Additional diode laser heterodyne measurements on ammonia. J Mol Spectrosc 1981;90:297–301.
[45] Urban Š, Špirko V, Papoušek D, Kauppinen J, Belov SP, Gershtein LI, et al. A simultaneous analysis of the microwave, submillimeter-wave, far infrared, and infrared-microwave two-photon transitions between the ground and $\nu_2$ inversion–rotation levels of $^{14}NH_3$. J Mol Spectrosc 1981;88:274–92.
[46] Sasada H, Hasegawa Y, Amano T, Shimizu T. High-resolution infrared and microwave spectroscopy of the $\nu_4$ and $2\nu_2$ bands of $^{14}NH_3$ and $^{15}NH_3$. J Mol Spectrosc 1982;96:106–30.
[47] Cohen EA, Weber WH, Poynter RL, Margolis JS. Observation of forbidden transitions in the $\nu_4$ band of $NH_3$: corrections to the ground state $\Delta K=3$ intervals. Mol Phys 1983;50:727–32.
[48] Ohtsu M, Kotani H, Tagawa H. Spectral measurements of $NH_3$ and $H_2O$ for pollutant gas monitoring by 1.5 μm InGaAsP/InP lasers. J Appl Phys 1983;22:1553.
[49] Spirko V. Vibrational anharmonicity and the inversion potential function of $NH_3$. J Mol Spectrosc 1983;101:30–47.

[50] Urban Š, Papoušek D, Kauppinen J, Yamada K, Winnewisser G. The $\nu_2$ band of $^{14}NH_3$: a calibration standard with better than $1\times10^{-4}$ cm$^{-1}$ precision. J Mol Spectrosc 1983;101:1–15.

[51] Poynter RL, Margolis JS. The $\nu_2$ spectrum of $NH_3$. Mol Phys 1984;51:393–412.

[52] Urban Š, D'Cunha R, Narahari Rao K, Papoušek D. The $\Delta k=\pm2$ "forbidden band" and inversion-rotation energy levels of ammonia. Can J Phys 1984;62:1775–91.

[53] Weber WH. Laser-Stark spectrum of $NH_3$ with the CO laser: determination of the ground state dipole moment. J Mol Spectrosc 1984;107:405–16.

[54] Brown LR, Toth RA. Comparison of the frequencies of $NH_3$, $CO_2$, $H_2O$, $N_2O$, CO, and $CH_4$ as infrared calibration standards. J Opt Soc Am B 1985;2:842–56.

[55] Kim K. Integrated infrared intensities in $NH_3$. J Quant Spectrosc Radiat Transf 1985;33:611–4.

[56] Urban Š, Misra P, Narahari Rao K. The $\nu_1+\nu_2$ and $\nu_1+\nu_2-\nu_2$ bands of $^{14}NH_3$ and $^{15}NH_3$. J Mol Spectrosc 1985;114:377–94.

[57] Coy SL, Lehmann KK. Rotational structure of ammonia N–H stretch overtones: five and six quanta bands. J Chem Phys 1986;84:5239–49.

[58] Hermanussen J, Bizzarri A, Baldacchini G. Diode laser measurements of ammonia absorption lines over the range 620–740 cm$^{-1}$. J Mol Spectrosc 1986;119:291–8.

[59] Papousek D, Urban Š, Špirko V, Narahari Rao K. The $\Delta k=\pm2$ and $\Delta k=\pm3$ forbidden transitions in the vibrational–rotational spectra of symmetric top molecules $NH_3$ and $H_3O^+$. J Mol Struct 1986;141:361–6.

[60] Sasada H, Schwendeman RH, Magerl G, Poynter RL, Margolis JS. High-resolution spectroscopy of the $v_2=2a\leftarrow v_2=1$ s band of $^{14}NH_3$. J Mol Spectrosc 1986;117:317–30.

[61] Ueda Y, Iwahori J. Laser Stark spectroscopy; a case study in the $\nu_2$ fundamental band of $^{14}NH_3$. J Mol Spectrosc 1986;116:191–213.

[62] Urban Š, D'Cunha R, Manheim J, Narahari Rao K. High-$J$ transitions in the $\nu_2$ bands of $^{14}NH_3$ and $^{15}NH_3$. J Mol Spectrosc 1986;118:298–309.

[63] Barth HD, Huisken F. CARS spectroscopy in supersonic jets of ammonia monomers and clusters. J Chem Phys 1987;87:2549–59.

[64] D'Cunha R. The $a2\nu_2\leftarrow s\nu_2$ bands of $^{14}NH_3$ and $^{15}NH_3$. J Mol Spectrosc 1987;122:130–4.

[65] Lellouch E, Lacome N, Guelachvili G, Tarrago G, Encrenaz T. Ammonia: experimental absolute linestrengths and self-broadening parameters in the 1800- to 2100-cm$^{-1}$. J Mol Spectrosc 1987;124:333–47.

[66] Tanaka K, Ito H, Tanaka T. $CO_2$ laser-microwave double resonance spectroscopy of $NH_3$: precise measurement of dipole moment in the ground state. J Chem Phys 1987;87:1557–67.

[67] Lehmann KK, Coy SL. Spectroscopy and intramolecular dynamics of highly excited vibrational states of $NH_3$. J Chem Soc Faraday Trans II 1988;84:1389–406.

[68] Snels M, Baldacchini G. Shape and width if IR absorption lines of ammonia expanded in a supersonic jet. Appl Phys B 1988;47:277–82.

[69] Tanaka K, Endo Y, Hirota E. Submillimeter-wave spectrum of $k=\pm1\leftarrow\mp2$ transitions of $NH_3$. Chem Phys Lett 1988;146:165–8.

[70] Coy SL, Lehmann KK. Modeling the rotational and vibrational structure of the i.r. optical spectrum of $NH_3$. Spectrochim Acta 1989;45A:47–56.

[71] Guelachvili G, Abdullah AH, Tu N, Narahari Rao K, Urban Š, Papoušek D. Analysis of high-resolution Fourier-transform spectra of $^{14}NH_3$ at 3.0 μm. J Mol Spectrosc 1989;133:345–64.

[72] Urban Š, Tu N, Narahari Rao K, Guelachvili G. Analysis of high-resolution Fourier transform spectra of $^{14}NH_3$ at 2.3 μm. J Mol Spectrosc 1989;133:312–30.

[73] Fusina L, Baldacchini G. The spectroscopic parameters of the $\nu_2=2a$ state for $^{14}NH_3$ and $^{15}NH_3$. J Mol Spectrosc 1990;141:23–8.

[74] Hepp M, Winnewisser G, Yamada KMT. Collisional nuclear spin intercombination in $NH_3$ observed in supersonic jet expansion by diode laser spectroscopy. J Mol Spectrosc 1992;153:376–84.

[75] Martin JML, Lee TJ, Taylor PR. An accurate ab initio quartic force field for ammonia. J Chem Phys 1992;97:8361–71.

[76] Sasada H, Endo Y, Hirota E, Poynter RL, Margolis JS. Microwave and Fourier-transform infrared spectroscopy of the $v_4$=1 and $v_2$=2 states of $NH_3$. J Mol Spectrosc 1992;151:33–53.

[77] Lundsberg-Nielsen L, Hegelund F, Nicolaisen FM. Analysis of the high-resolution spectrum of ammonia ($^{14}NH_3$) in the near-infrared region, 6400–6900 cm$^{-1}$. J Mol Spectrosc 1993;162:230–45.

[78] Markov VN, Pine AS, Buffa G, Tarrini O. Self broadening in the $\nu_1$ band of $NH_3$. J Quant Spectrosc Radiat Transf 1993;50:167–78.

[79] Pine AS, Dang-Nhu M. Spectral intensities in the $\nu_1$ band of $NH_3$. J Quant Spectrosc Radiat Transf 1993;50:565–70.

[80] Wu T, An H, Jiang P, Fang Y, Tao S, Ye P. Spectral measurement of $NH_3$ absorption lines by a 1.5 μm grating-external-cavity semiconductor laser. Opt Lett 1993;18:729.

[81] Brown LR, Peterson DB. An empirical expression for linewidths of ammonia from far-infrared measurements. J Mol Spectrosc 1994;168:593–606.

[82] Chu Z, Chen L, Cheo PK. Absorption spectra of $NH_3$ using a microwave-sideband $CO_2$-laser spectrometer. J Quant Spectrosc Radiat Transf 1994;51:591–602.

[83] Kauppi E, Halonen L. Five-dimensional local mode-Fermi resonance model for overtone spectra of ammonia. J Chem Phys 1995;103:6861–72.

[84] Kleiner I, Tarrago G, Brown LR. Positions and intensities in the $3\nu_2/\nu_2+\nu_4$ vibrational system of $^{14}NH_3$ near 4 μm. J Mol Spectrosc 1995;173:120–45.

[85] Brown LR, Margolis JS. Empirical line parameters of $NH_3$ from 4791 to 5294 cm$^{-1}$. J Quant Spectrosc Radiat Transf 1996;56:283–94.

[86] Krupnov AF, Tretyakov MY, Bogey M, Bailleux S, Walters A, Delcroix B, et al. Microwave measurements of $J=2\leftarrow1, K=0,1$ ammonia transitions at 1.215 THz. J Mol Spectrosc 1996;176:442–3.

[87] Sarka K, Schötter HW. Effective Hamiltonian for rotation–inversion states of ammonia-like molecules. J Mol Spectrosc 1996;179:195–204.

[88] Marshall MD, Izgi KC, Muenter JS. IR-microwave double resonance studies of dipole moments in the $\nu_1$ and $\nu_3$ states of ammonia. J Chem Phys 1997;107:1037–44.

[89] Rush DJ, Wiberg KB. Ab initio CBS-QCI calculations of the inversion mode of ammonia. J Phys Chem A 1997;101:3143–51.

[90] Behrens M, Buck U, Fröchtenicht R, Hartmann M, Huisken F, Rohmund F. Rotationally resolved IR spectroscopy of ammonia trapped in cold helium clusters. J Chem Phys 1998;109:5914–20.

[91] Belov SP, Urban Š, Winnewisser G. Hyperfine structure of rotation–inversion levels in the excited $\nu_2$ state of ammonia. J Mol Spectrosc 1998;189:1–7.

[92] Fichoux H, Khelkhal M, Rusinek E, Legrand J, Herlemont F, Urban Š. Double resonance sub-Doppler study of the allowed and $\Delta K=-3$ forbidden $Q(3,3)$ transitions to the $\nu_2$ vibrational state of $^{14}NH_3$. J Mol Spectrosc 1998;192:169–78.

[93] Berden G, Peeters R, Meijer G. Cavity-enhanced absorption spectroscopy of the 1.5 μm band system of jet-cooled ammonia. Chem Phys Lett 1999;307:131–8.

[94] Fabian M, Yamada KMT. Absolute intensity of the $NH_3$ $\nu_2$ band. J Mol Spctrosc 1999;198:102–9.

[95] Kleiner I, Brown LR, Tarrago G, Kou Q-L, Picqué N, Guelachvili G, et al. Positions and intensities in the $2\nu_4/\nu_1/\nu_3$ vibrational system of $^{14}NH_3$ near 3 μm. J Mol Spectrosc 1999;193:46–71.

[96] Cottaz C, Kleiner I, Tarrago G, Brown LR, Margolis JS, Poynter RL, et al. Line positions and intensities in the $2\nu_2/\nu_4$ vibrational system of $^{14}NH_3$ near 5–7 μm. J Mol Spectrosc 2000;203:285–309.

[97] Fouchet T, Lellouch E, Bézard B, Encrenaz T, Drossart P, Feuchtgruber H, et al. ISO-SWS observations of Jupiter: measurement of the ammonia tropospheric profile and of the $^{15}N/^{14}N$ isotopic ratio. Icarus 2000;143:223–43.

[98] Urban Š, Herlemont F, Khelkhal M, Fichoux H, Legrand J. High-accuracy determination of the frequency and quadrupole structure of the $sP(1,0)$ and $aR(0,0)$ transitions to the $\nu_2$ state of $^{14}NH_3$. J Mol Spectrosc 2000;200:280–2.

[99] Cottaz C, Tarrago G, Kleiner I, Brown LR. Assignments and intensities of $^{14}NH_3$ hot bands in the 5- to 8−μm ($3\nu_2-\nu_2,\nu_2+\nu_4-\nu_2$) and 4−μm ($4\nu_2-\nu_2,\nu_1-\nu_2,\nu_3-\nu_2$ and $2\nu_4-\nu_2$) regions. J Mol Spectrosc 2001;209:30–49.

[100] Klopper W, Samson CCM, Tarczay G, Császár AG. Equilibrium inversion barrier of $NH_3$ from extrapolated coupled-cluster pair energies. J Comput Chem 2001;22:1306–14.

[101] Webber ME, Baer DS, Hanson RK. Ammonia monitoring near 1.5 μm with diode-laser absorption sensors. Appl Opt 2001;40:2031–42.

[102] Lin H, Thiel W, Yurchenko SN, Carvajal M, Jensen P. Vibrational energies for $NH_3$ based on high level *ab initio* potential energy surfaces. J Chem Phys 2002;117:11265–76.

[103] Rajamäki T, Miani A, Halonen L. Six-dimensional *ab initio* potential energy surfaces for $H_3O^+$ and $NH_3$: approaching the subwavenumber accuracy for the inversion splittings. J Chem Phys 2003;118:10929–38.

[104] Leonard C, Carter S, Handy NC. The barrier to inversion of ammonia. Chem Phys Lett 2003;370:360–5.

[105] Gibb JS, Hancock G, Peverall R, Ritchie GAD, Russell LJ. Diode laser based detection and determination of pressure-induced

broadening coefficients in the $\nu_1+\nu_3$ combination band of ammonia. Eur Phys J D 2004;28:59–66.
[106] Lauvergnat D, Nauts A. A harmonic adiabatic approximation to calculate vibrational states of ammonia. Chem Phys 2004;305:105.
[107] Rajamäki T, Kállay M, Noga T, Valiron P, Halonen L. High excitations in coupled-cluster series: vibrational energy levels of ammonia. Mol Phys 2004;102:2297–310.
[108] Xu L-H, Liu Z, Yakovlev I, Tretyakov MY, Lees RM. External cavity tunable diode laser $NH_3$ spectra in the 1.5 μm region. Infrared Phys Techn 2004;45:31–45.
[109] Marquardt R, Sagui K, Klopper W, Quack M. Global analytical potential energy surface for large amplitude motions in ammonia. J Phys Chem B 2005;109:8439–51.
[110] Yurchenko SN, Carvajal M, Lin H, Zheng J, Thiel W, Jensen P. Dipole moment and rovibrational intensities in the electronic ground state of $NH_3$: bridging the gap between *ab initio* theory and spectroscopic experiment. J Chem Phys 2005;122:104317.
[111] Yurchenko SN, Zheng J, Lin H, Jensen P, Thiel W. Potential energy surface for the electronic ground state of $NH_3$ up to 20 000 $cm^{-1}$ above equilibrium. J Chem Phys 2005;123:134308.
[112] Chen P, Pearson JC, Pickett HM, Matsuura S, Blake GA. Measurements of $^{14}NH_3$ in the $\nu_2=1$ state by a solid-state, photomixing, THz spectrometer, and a simultaneous analysis of the microwave, terahertz, and infrared transitions between the ground and $\nu_2$ inversion–rotation levels. J Mol Spectrosc 2006;236:116–26.
[113] Coudert LH, Roueff E. Linelists for $NH_3$, $NH_2D$, $ND_2H$, and $ND_3$ with quadrupole coupling hyperfine components. Astron Astrophys 2006;449:855–9.
[114] Pirali O, Vervloet M. Far-infrared Fourier transform emission spectroscopy in the gas phase. Chem Phys Lett 2006;423:376–81.
[115] Li L, Lees RM, Xu L-H. External cavity tunable diode laser spectra of the $\nu_1+2\nu_4$ stretch-band combination bands of $^{14}NH_3$ and $^{15}NH_3$. J Mol Spectrosc 2007;243:219–26.
[116] Bethlem HL, Kajita M, Sartakov B, Meijer G, Ubachs W. Prospects for precision measurements on ammonia molecules in a fountain. Eur Phys J D 2008;163:55–69.
[117] Cubillas AM, Hald J, Petersen JC. High resolution spectroscopy of ammonia in a hollow-core fibre. Opt Express 2008;16:3976–85.
[118] Huang X, Schwenke DW, Lee TJ. An accurate global potential energy surface, dipole moment surface, and rovibrational frequencies for $NH_3$. J Chem Phys 2008;129:214304.
[119] Lees RM, Li L, Xu L-H. New VISTA on ammonia in the 1.5 μm region: assignments for the $\nu_3+2\nu_4$ bands of $^{14}NH_3$ and $^{15}NH_3$ by isotopic shift labeling. J Mol Spectrosc 2008;251:241–51.
[120] O'Leary DM, Orphal J, Ruth AA, Heitmann U, Chelin P, Fellows CE. The cavity-enhanced absorption spectrum of $NH_3$ in the near-infrared region between 6856 and 7000 $cm^{-1}$. J Quant Spectrosc Radiat Transf 2008;109:1004–15.
[121] Puzzarini C. Ab initio characterization of $XH_3$ (X = N,P). Part II. Electric, magnetic and spectroscopic properties of ammonia and phosphine. Theor Chem Acc 2008;121:1–10.
[122] Cacciani P, Cosleou J, Khelkhal M, Tudorie M, Puzzarini C, Pracna P. Nuclear spin conversion in $NH_3$. Phys Rev A 2009;80:042507.
[123] Cazzoli G, Dore L, Puzzarini C. The hyperfine structure of the inversion–rotation transition $J_K=1_0\leftarrow0_0$ of $NH_3$ investigated by Lamb-dip spectroscopy. Astron Astrophys 2009;507:1707–10.
[124] Czajkowski A, Alcock AJ, Bernard JE, Madej AA, Corrigan M, Chepurov S. Studies of saturated absorption and measurements of optical frequency for lines in the $\nu_1+\nu_3$ and $\nu_1+2\nu_4$ bands of ammonia at 1.5 micron. Opt Express 2009;17:9258–69.
[125] Jia H, Zhao W, Cai T, Chen W, Zhang W, Gao X. Absorption spectroscopy of ammonia between 6526–6538 $cm^{-1}$. J Quant Spectrosc Radiat Transf 2009;110:347–56.
[126] Yurchenko SN, Barber RJ, Yachmenev A, Thiel W, Jensen P, Tennyson J. A variationally computed $T=300$ K line list for $NH_3$. J Phys Chem A 2009;113:11845–55.
[127] Li YQ, Varandas AJC. Ab-initio-based global many-body expansion potential energy surface for the electronic ground state of the ammonia molecule. J Phys Chem A 2010;114:6669–80.
[128] Petersen JC, Hald J. Microwave optical double resonance spectroscopy of ammonia in a hollow-core fiber. Opt Express 2010;18:7955–64.
[129] Yu S, Pearson JC, Drouin BJ, Sung K, Pirali O, Vervloet M, et al. Submillimeter-wave and far-infrared spectroscopy of high-$J$ transitions of the ground and $\nu_2=1$ states of ammonia. J Chem Phys 2010;133(17):174317.
[130] Drouin BJ, Yu S, Pearson JC, Gupta H. Terahertz spectroscopy for space applications: 2.5–2.7 THz spectra of HD, $H_2O$ and $NH_3$. J Mol Struct 2011;1006:2–12.
[131] Fábri C, Mátyus E, Császár AG. Rotating full- and reduced-dimensional quantum chemical models of molecules. J Chem Phys 2011;134:074105.
[132] Guinet M, Jeseck P, Mondelain D, Pepin I, Janssen C, Camy-Peyret C, et al. Absolute measurements of intensities, positions and self-broadening coefficients of R branch transitions in the $\nu_2$ band of ammonia. J Quant Spectrosc Rad Transf 2011;112:1950–60.
[133] Huang X, Schwenke DW, Lee TJ. Rovibrational spectra of ammonia. I. Unprecedented accuracy of a potential energy surface used with nonadiabatic corrections. J Chem Phys 2011;134:044320.
[134] Yurchenko SN, Barber RJ, Tennyson J, Thiel W, Jensen P. Toward efficient refinement of molecular potential energy surfaces: ammonia as a case study. J Mol Spectrosc 2011;268:123–9.
[135] Zobov NF, Shirin SV, Ovsyannikov RI, Polyansky OL, Yurchenko SN, Barber RJ, et al. Analysis of high temperature ammonia spectra from 780 to 2100 $cm^{-1}$. J Mol Spectrosc 2011;269:104–8.
[136] Lemarchand C, Triki M, Darquie B, Borde CJ, Chardonnet C, Daussy C. Progress towards an accurate determination of the Boltzmann constant by Doppler spectroscopy. New J Phys 2011;13:073028.
[137] Hargreaves RJ, Li G, Bernath PF. Ammonia line lists from 1650 to 4000 $cm^{-1}$. J Quant Spectrosc Radiat Transf 2012;113:670–9.
[138] Hargreaves RJ, Li G, Bernath PF. Hot $NH_3$ spectra for astrophysical applications. Astrophys J 2012;735:111.
[139] Cacciani P, Cermak P, Cosléou J, Khelkhal M, Jeseck P, Michaut X. New progress in spectroscopy of ammonia in the infrared range using evolution of spectra from 300 K down to 122 K. J Quant Spectrosc Radiat Transf 2012;113:1084–91.
[140] Sung K, Brown LR, Huang X, Schwenke DW, Lee TJ, Coy SL, et al. Extended line positions, intensities, empirical lower state energies and quantum assignments of $NH_3$ from 6300 to 7000 $cm^{-1}$. J Quant Spectrosc Radiat Transf 2012;113:1066–83.
[141] Triki M, Lemarchand C, Darquie B, Sow PLT, Roncin V, Chardonnet C, et al. Speed-dependent effects in $NH_3$ self-broadened spectra: towards the determination of the Boltzmann constant. Phys Rev A 2012;85:062510.
[142] Down MJ, Hill C, Yurchenko SN, Tennyson J, Brown LR, Kleiner I. Re-analysis of ammonia spectra: updating the HITRAN $^{14}NH_3$ database. J Quant Spectrosc Radiat Transf 2013;130:260–72.
[143] Lemarchand C, Mejri S, Sow PLT, Triki M, Tokunaga SK, Briaudeau S, et al. A revised uncertainty budget for measuring the Boltzmann constant using the Doppler broadening technique on ammonia. Metrologica 2013;50:623–30.
[144] Marquardt R, Sagui K, Zheng J, Thiel W, Luckhaus D, Yurchenko S, et al. Global analytical potential energy surface for the electronic ground state of $NH_3$ from high level ab initio calculations. J Phys Chem A 2013;117:7502–22.
[145] Cacciani P, Cermák P, Cosléou J, El Rohm J, Hovorka J, Khelkhal M. Spectroscopy of ammonia in the range 6626–6805 $cm^{-1}$: using temperature dependence towards a complete list of lower state energy transitions. Mol Phys 2014;112:2476–85.
[146] Cermák P, Hovorka J, Veis P, Cacciani P, Cosléou J, Romh JE, et al. Spectroscopy of $^{14}NH_3$ and $^{15}NH_3$ in the 23 μm spectral range with a new VECSEL laser source. J Quant Spectrosc Radiat Transf 2014;137:13–22.
[147] Dietiker P, Milogyadov E, Quack M, Schneider A, Seyfang G. Two photon IR-laser induced population transfer in $NH_3$ - First steps to measure parity violation in chiral molecules. In: Stock PSD, Wester R, editors. Proceedings of the 19th symposium on atomic, cluster and surface physics 2014 (SASP 2014). Insbruck: Innsbruck University Press; 2014.
[148] Földes T, Golebiowski D, Herman M, Softley TP, di Lonardo G, Fusina L. Low-temperature high-resolution absorption spectrum of $^{14}NH_3$ in the $\nu_1+\nu_3$ band region (1.51 μm). Mol Phys 2014;112:2407–18.
[149] Sow PLT, Mejri S, Tokunaga SK, Lopez O, Goncharov A, Argence B, et al. A widely tunable 10−μm quantum cascade laser phase-locked to a state-of-the-art mid-infrared reference for precision molecular spectroscopy. Appl Phys Lett 2014;104:264101.
[150] Császár AG, Allen WD, Schaefer III HF. In pursuit of the *ab initio* limit for conformational energy prototypes. J Chem Phys 1998;108:9751–64.
[151] Császár AG, Tarczay G, Leininger ML, Polyansky OL, Tennyson J, Allen WD. Dream or reality: complete basis set full configuration interaction potential energy hypersurfaces. In: Demaison J, Sarka K, editors. Spectroscopy from space. Dordrecht: Kluwer; 2001. p. 317–39.
[152] Császár AG, Fábri C, Szidarovszky T, Mátyus E, Furtenbacher T, Czakó G. Fourth age of quantum chemistry: molecules in motion. Phys Chem Chem Phys 2012;14:1085–106.
[153] Mátyus E, Czakó G, Sutcliffe B, Császár AG. Variational vibrational calculations with arbitrary potentials using the Eckart–Watson

Hamiltonians and the discrete variable representation. J Chem Phys 2007;127:084102.
[154] Yurchenko SN, Thiel W, Jensen P. Theoretical ROVibrational energies (TROVE): a robust numerical approach to the calculation of rovibrational energies for polyatomic molecules. J Mol Spectrosc 2007;245:126–40.
[155] Mátyus E, Šimunek J, Császár AG. On variational computation of a large number of vibrational energy levels and wave functions for medium-sized molecules. J Chem Phys 2009;131:074106.
[156] Mátyus E, Czakó G, Császár AG. Toward black-box-type full- and reduced-dimensional variational (ro)vibrational computations. J Chem Phys 2009;130:134112.
[157] Bunker PR, Jensen P. Molecular symmetry and spectroscopy. NRC Research; 1998.
[158] Owens A, Yurchenko SN, Thiel W, Špirko V. Prediction of the $^{14}NH_3$ and $^{15}NH_3$ probes of a variable proton-to-electron mass ratio. J Phys Chem Lett (accepted for publication).
[159] Császár AG, Czakó G, Furtenbacher T, Mátyus E. An active database approach to complete spectra of small molecules. Annu Rep Comput Chem 2007;3:155–76.
[160] Császár AG, Furtenbacher T. Spectroscopic networks. J Mol Spectrosc 2011;266:99–103.
[161] Furtenbacher T, Császár AG, Tennyson J. MARVEL: measured active rotational–vibrational energy levels. J Mol Spectrosc 2007;245:115–25.
[162] Furtenbacher T, Császár AG. On employing $H_2{}^{16}O$, $H_2{}^{17}O$, $H_2{}^{18}O$, and $D_2{}^{16}O$ lines as frequency standards in the 15–170 $cm^{-1}$ window. J Quant Spectrosc Radiat Transf 2008;109:1234–51.
[163] Furtenbacher T, Császár AG. MARVEL: measured active rotational-vibrational energy levels. II. Algorithmic improvements. J Quant Spectrosc Radiat Transf 2012;113:929–35.
[164] Tennyson J, Bernath PF, Brown LR, Campargue A, Carleer MR, Császár AG, et al. IUPAC critical evaluation of the rotational–vibrational spectra of water vapor. Part I. Energy levels and transition wavenumbers for $H_2{}^{17}O$ and $H_2{}^{18}O$. J Quant Spectrosc Radiat Transf 2009;110:573–96.
[165] Tennyson J, Bernath PF, Brown LR, Campargue A, Carleer MR, Császár AG, et al. IUPAC critical evaluation of the rotational–vibrational spectra of water vapor. Part II. Energy levels and transition wavenumbers for $HD^{16}O$, $HD^{17}O$, and $HD^{18}O$. J Quant Spectrosc Radiat Transf 2010;111:2160–84.
[166] Tennyson J, Bernath PF, Brown LR, Campargue A, Carleer MR, Császár AG, et al. IUPAC critical evaluation of the rotational–vibrational spectra of water vapor. Part III. Energy levels and transition wavenumbers for $H_2{}^{16}O$. J Quant Spectrosc Radiat Transf 2013;117:29–80.
[167] Tennyson J, Bernath PF, Brown LR, Campargue A, Császár AG, Daumont L, et al. IUPAC critical evaluation of the rotational–vibrational spectra of water vapor. Part IV. Energy levels and transition wavenumbers for $D_2{}^{16}O$, $D_2{}^{17}O$ and $D_2{}^{18}O$. J Quant Spectrosc Radiat Transf 2014;142:93–108.
[168] Tennyson J, Bernath PF, Brown LR, Campargue A, Császár AG, Daumont L, et al. A database of water transitions from experiment and theory (IUPAC Technical Report). Pure Appl Chem 2014;86:71–83.
[169] Furtenbacher T, Szidarovszky T, Fábri C, Császár AG. MARVEL analysis of the rotational–vibrational states of the molecular ions $H_2D^+$ and $D_2H^+$. Phys Chem Chem Phys 2013;15:10181–93.
[170] Furtenbacher T, Szidarovszky T, Mátyus E, Fábri C, Császár AG. Analysis of the rotational–vibrational states of the molecular ions $H_3^+$. J Chem Theory Comput 2013;9:5471–8.
[171] Fábri C, Mátyus E, Furtenbacher T, Mihály B, Zoltáni T, Nemes L, et al. Analysis of the rotational–vibrational states of the molecular ions $H_3^+$. J Chem Phys 2011;135:094307.
[172] Furtenbacher T, Árendás P, Mellau G, Császár AG. Simple molecules as complex systems. Sci Rep 2014;4:4654.
[173] Watson JKG. Robust weighting in least-squares fits. J Mol Spectrosc 2003;219:326–8.
[174] Yurchenko SN, Barber RJ, Tennyson J. A variationally computed hot line list for $NH_3$. Mon Not R Astron Soc 2011;413:1828–34.
[175] Hougen JT. Classification of rotational energy levels for symmetric-top molecules. J Chem Phys 1962;37:1433–41.
[176] Yurchenko SN, Barber RJ, Yachmenev A, Thiel W, Jensen P, Tennyson J. A variationally computed $T=300$ K line list for $NH_3$. J Phys Chem A 2009;113:11845–55.
[177] Yurchenko SN. A theoretical room-temperature line list for $^{15}NH_3$. J Quant Spectrosc Radiat Transf 2015;152:28–36.
[178] Yurchenko SN, Barber RJ, Tennyson J, Thiel W, Jensen P. Towards efficient refinement of molecular potential energy surfaces: ammonia as a case study. J Mol Spectrosc 2011;268:123–9.
[179] Huang X, Schwenke DW, Lee TJ. Rovibrational spectra of ammonia. I. Unprecedented accuracy of a potential energy surface used with nonadiabatic corrections. J Chem Phys 2011;134:044320.
[180] Huang X, Schwenke DW, Lee TJ. Rovibrational spectra of ammonia. II. Detailed analysis, comparison, and prediction of spectroscopic assignments for $^{14}NH_3$, $^{15}NH_3$, and $^{14}ND_3$. J Chem Phys 2011;134:044321.
[181] Marquardt R, Quack M, Thanopulos I, Luckhaus D. A global electric dipole function of ammonia and isotopomers in the electronic ground state. J Chem Phys 2003;119:10724.
[182] Chen P, Pearson JC, Pickett HM, Matsuura S, Blake GA. Measurements of $^{14}NH_3$ in the state by a solid-state, photomixing, THz spectrometer, and a simultaneous analysis of the microwave, terahertz, and infrared transitions between the ground and inversion-rotation levels. J Mol Spectrosc 2006;36:116–26.
[183] Angstl R, Finsterholzl H, Frunder H, Illig D, Papoušek D, Pračn P, et al. Fourier transform and CARS spectroscopy of the $\nu_1$ and $\nu_3$ fundamental bands of $^{14}NH_3$. J Mol Spectrosc 1985;114:454–72.
[184] Rothman LS, Gordon IE, Babikov Y, Barbe A, Benner DC, Bernath PF, et al. The *HITRAN* 2012 molecular spectroscopic database. J Quant Spectrosc Radiat Transf 2013;130:4–50. http://dx.doi.org/10.1016/jqsrt.2013.07.002.
[185] Rothman LS, Jacquemart D, Barbe A, Benner DC, Birk M, Brown LR, et al. The *HITRAN* 2004 molecular spectroscopic database. J Quant Spectrosc Radiat Transf 2005;96:139–204.
[186] Rothman LS, Gordon IE, Barbe A, Benner DC, Bernath PF, Birk M, et al. The *HITRAN* 2008 molecular spectroscopic database. J Quant Spectrosc Radiat Transf 2009;110:533–72.
[187] Yurchenko SN, Zheng J, Lin H, Jensen P, Thiel W. Potential energy surface for the electronic ground state of $NH_3$ up to 20 000 $cm^{-1}$ above equilibrium. J Chem Phys 2005;123:134308.
[188] Barton EJ, Yurchenko SN, Tennyson J, Fateev A. High-resolution absorption measurements of $NH_3$ at high temperatures: 600–2100 $cm^{-1}$. J Quant Spectrosc Radiat Transf submitted for publication, 2015.
[189] Herzberg G. Molecular spectra and molecular structure, vols. 1–3. Melbourne: Van Nostrand Reinhold; 1945.